

# SUPPORTING INFORMATION

## **Photoinduced dynamics of oxyluciferin analogues: Unusual enol “super”photoacidity and evidence for keto-enol isomerization**

Kyril M. Solntsev, Sergey P. Laptanok, Panče Naumov

School of Chemistry and Biochemistry, Georgia Institute of Technology, 901 Atlantic Drive,  
Atlanta, Georgia 30332-0400, USA

Laboratory for Optical Biosciences, CNRS, Ecole Polytechnique, 91128 Palaiseau, France

INSERM U696, 91128 Palaiseau, France,

New York University Abu Dhabi, PO Box 129188, Abu Dhabi, UAE

Institute for Chemical Research and the Young Researcher Development Center, Kyoto  
University, Uji, Kyoto 611-0011, Japan

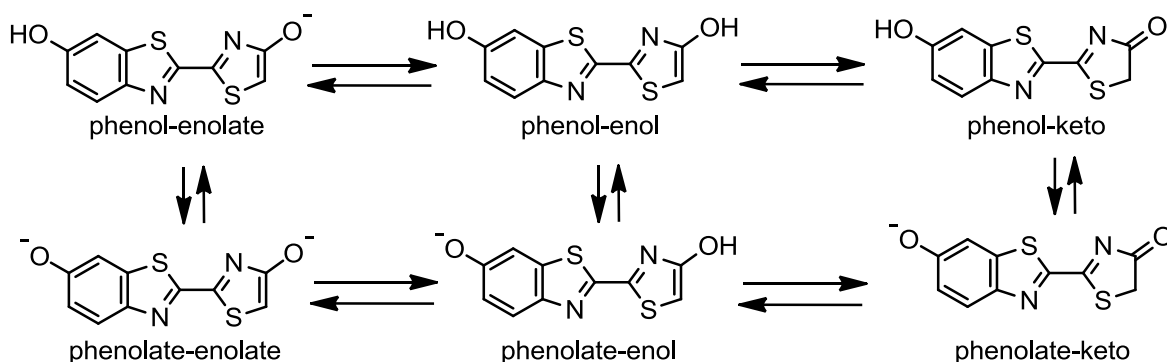


**Chart S1.** The six possible chemical forms of firefly oxyluciferin and their equilibria.

### Time-correlated single photon counting spectroscopy

Fluorescence lifetimes were measured using an Edinburgh Instruments time-correlated single photon counting (TCSPC) system. In these measurements, picosecond excitation pulses diode lasers (Picoquant) emitting at 372 nm or 467 nm was used as an excitation light source. The detection system consisted of a high speed MicroChannel Plate PhotoMultiplier Tube (MCP-PMT, Hamamatsu R3809U-50) and TCSPC electronics. The time resolution of the system was 40 ps after deconvolution with an IRF signal.

### Global and target analysis.

The aim of the analysis is to obtain a model-based description of the time-resolved data in terms of a small number of precisely estimated rate constants and fluorescence spectra. This was achieved by global analysis. The basis for global analysis is the superposition principle, which uses the assumption that the measured data result from a linear combination of  $n_{comp}$  components, each with a distinct time profile and spectrum. Mathematically the problem can be described as following:

$$\Psi(\lambda, t) = \sum_{i=1}^{n_{comp}} c_i(t) \epsilon_i(\lambda) \quad (1)$$

Global analysis was applied in two ways: Firstly, the data were fitted to a parallel model, in which  $n_{comp}$  excited species decay mono-exponentially in parallel. In this procedure, spectral shapes are left unconstrained yielding Decay Associated Spectra (DAS).

In this case the problem of equation 1 then described as:

$$\Psi(\lambda, t) = \sum_{i=1}^{n_{comp}} c_i^{DAS}(t, \theta) DAS_i(\lambda) \quad (2)$$

Where  $c_i^{DAS}(t, \theta)$  is the exponentially decaying concentration of component  $i$  convolved with the IRF. More complicated concentrations are linear combinations of these c DAS They are often described as compartmental models.<sup>1, 2</sup> In a sequential or unbranched unidirectional model the

<sup>1</sup>Godfrey, K. (1983). Compartmental Models and Their Application. Academic Press, London.

associated spectra are called evolution associated spectra (EAS), and the model of equation (1) then described as:

$$\Psi(\lambda, t) = \sum_{i=1}^{n_{comp}} c_i^{EAS}(t, \theta) EAS_i(\lambda) \quad (3)$$

With successively increasing lifetimes the EAS visualize the spectral evolution.

The data can be fitted to a full compartmental scheme is termed a target model, and this type of global analysis is referred to as target analysis. The target model, inspired by scientific hypotheses and assumptions, includes all possible branching routes and equilibria between compartments. With a target model it's possible to estimating the spectra of each of the excited species and associated spectra are called species associated spectra (SAS). The model of equation (1) in that case described as:

$$\Psi(\lambda, t) = \sum_{i=1}^{n_{comp}} c_i^{SAS}(t, \theta) SAS_i(\lambda) \quad (4)$$

Both  $c_i^{EAS}(t, \theta)$  and  $c_i^{SAS}(t, \theta)$  are linear combinations of all  $c_i^{DAS}(t, \theta)$ . Thus from the EAS or SAS new DAS can be computed, which obey the assumptions of the kinetic model used.

For more details about the use of compartmental models for global and target analysis of time-resolved spectroscopy data see reviews by van Stokkum and co-workers.<sup>3</sup> For details on parameter estimation techniques see Refs. 4 and 5.

---

<sup>2</sup>Bates, D. M.; Watts, D. G. (1988). Nonlinear regression analysis and its applications. John Wiley & Sons, New York.

<sup>3</sup>van Stokkum, I. H. M.; Larsen, D. S.; van Grondelle, R. *Biochim. Biophys. Acta.* **2004**, 1657, 82-104.

<sup>4</sup>Mullen, K. M.; van Stokkum, I. H. M. *J. Stat. Soft.* **2007**, 18, 1-46.

<sup>5</sup>van Stokkum, I. H. M.; Bal, H. E. *Concurrency and Computation-Practice & Experience* **2006**, 18, 263-269.

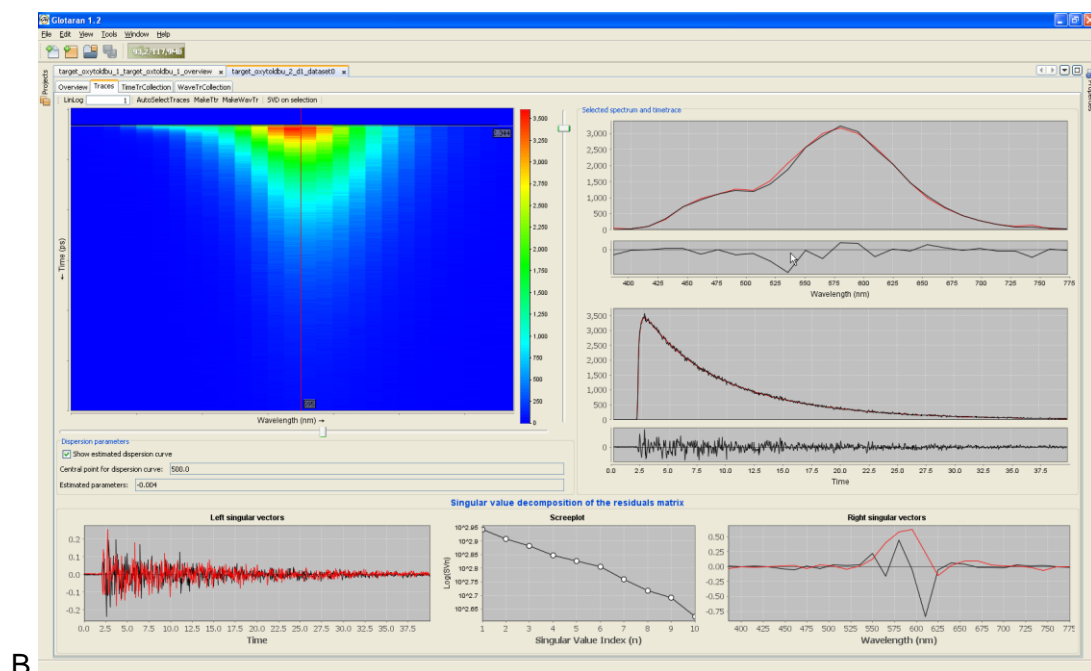
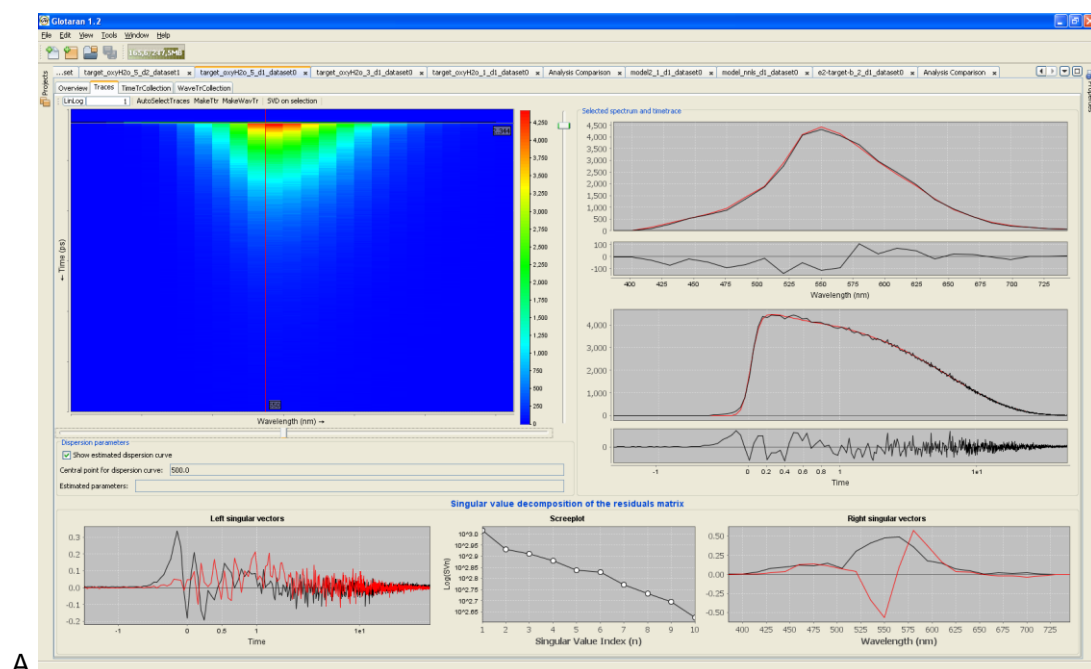


**Figure S1.** Screenshot of the fitting of spectra of **OxyLH<sub>2</sub>** in water (A) and **OxyLH<sub>2</sub>** in toluene/DBU (B) using the Glotaran software. 2D projection of the decay surface (upper left corner); selected spectral and time slices (black curves, right column graphs) together with the global fit curves (red curves of the same graphs), singular value decomposition of the residual matrix (lower graphs) as measure of the fit quality of the whole dataset<sup>4,5</sup> (also see ref. 34 in the main text for more details).

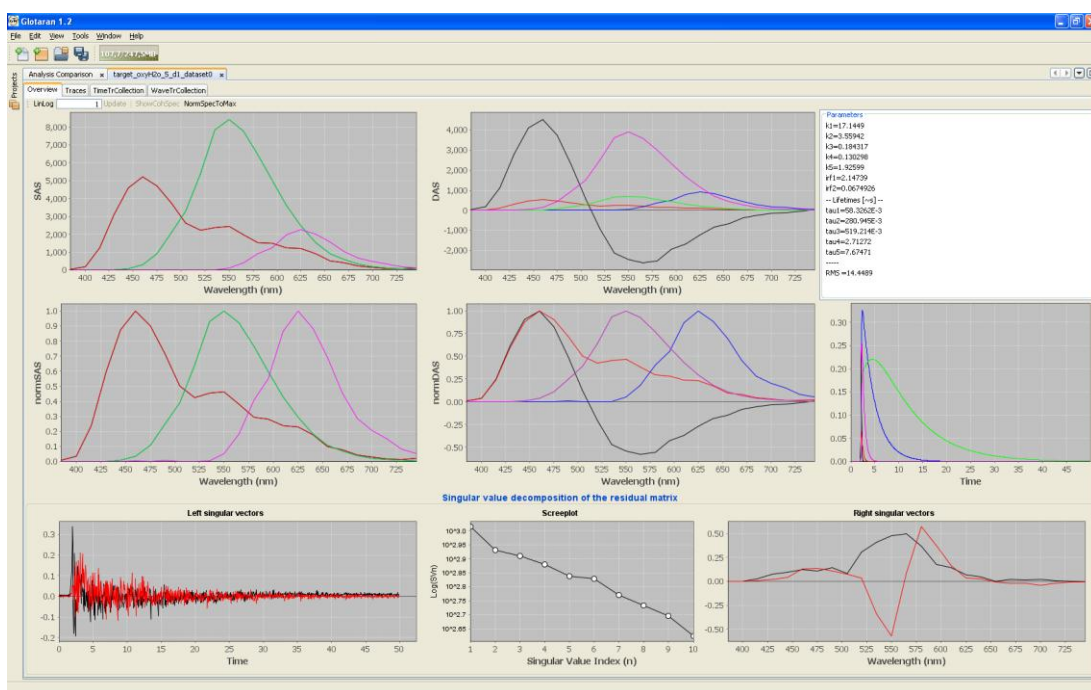


**Figure S2.** Screenshot of the fitting of spectra of **OxyLH<sub>2</sub>** in water using the Glotaran software. Relative (top row) and normalized (middle row) SAS, DAS; decays of the kinetic components (mid row, right graph); statistical analysis (bottom row).

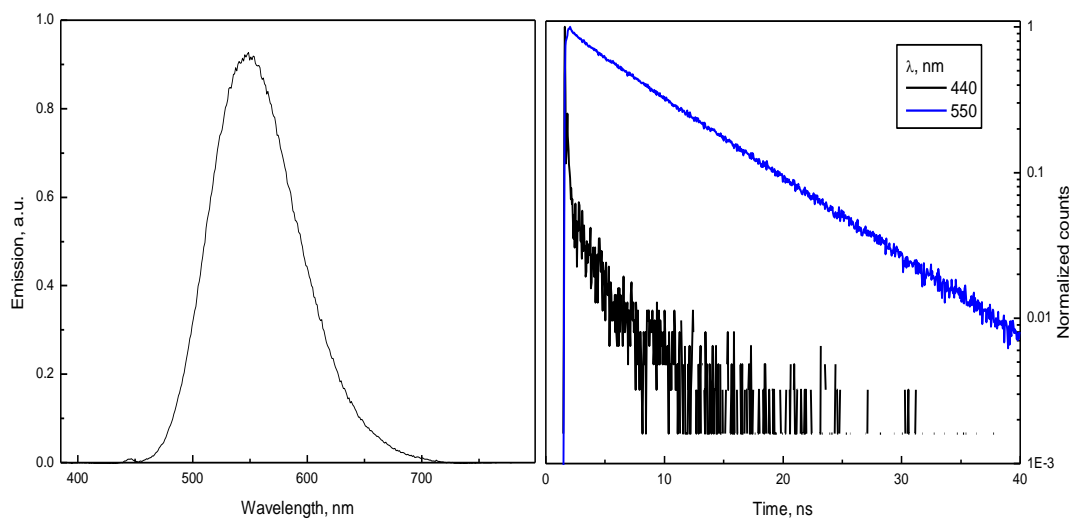


**Figure S3.** Steady-state (left) and time-resolved (right) emission of **HOxyLH** in  $H_2O$ . In both cases the samples were excited at 372 nm.

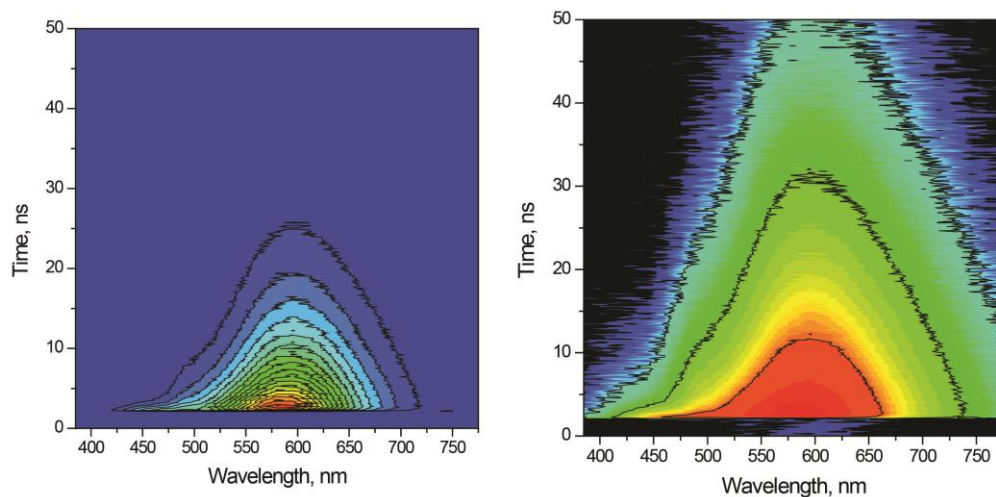


**Figure S4.** Fluorescence decay surface of **OxyLH<sub>2</sub>** in toluene /DBU after 372 nm laser excitation, with intensities plotted on a linear scale (left) and on log scale (right). The red color corresponds to stronger intensities.

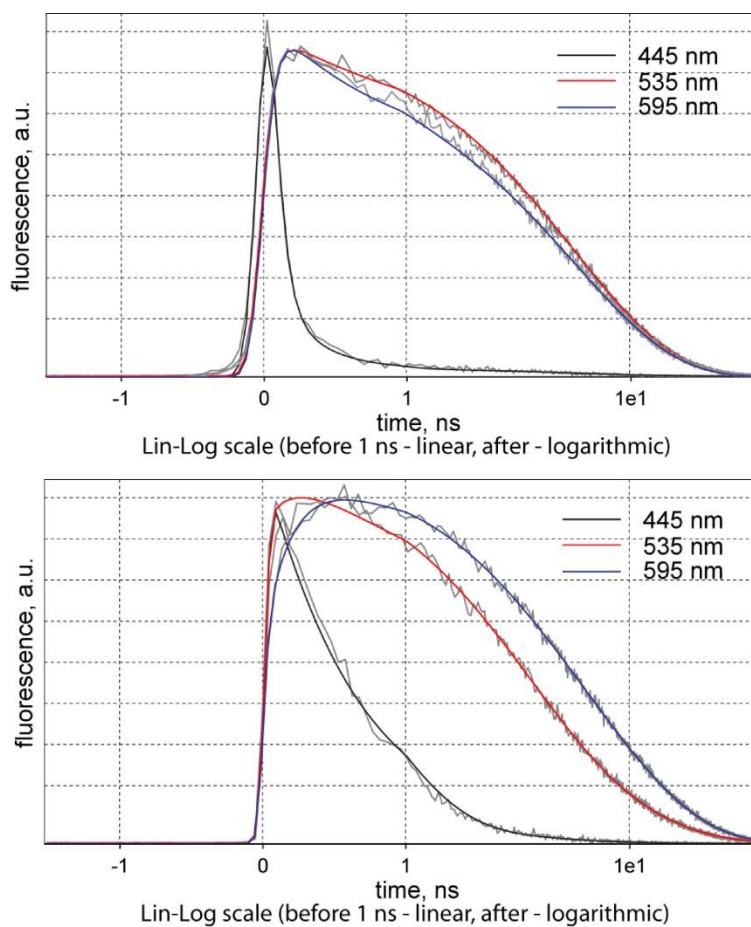


**Figure S5.** Kinetic traces of **OxyLH<sub>2</sub>** in water (top) and toluene/DBU (bottom) after 372 nm pulsed laser excitation recorded at various wavelengths. Gray lines represent the raw data, colored lines correspond to the fits derived from the global/target analysis.

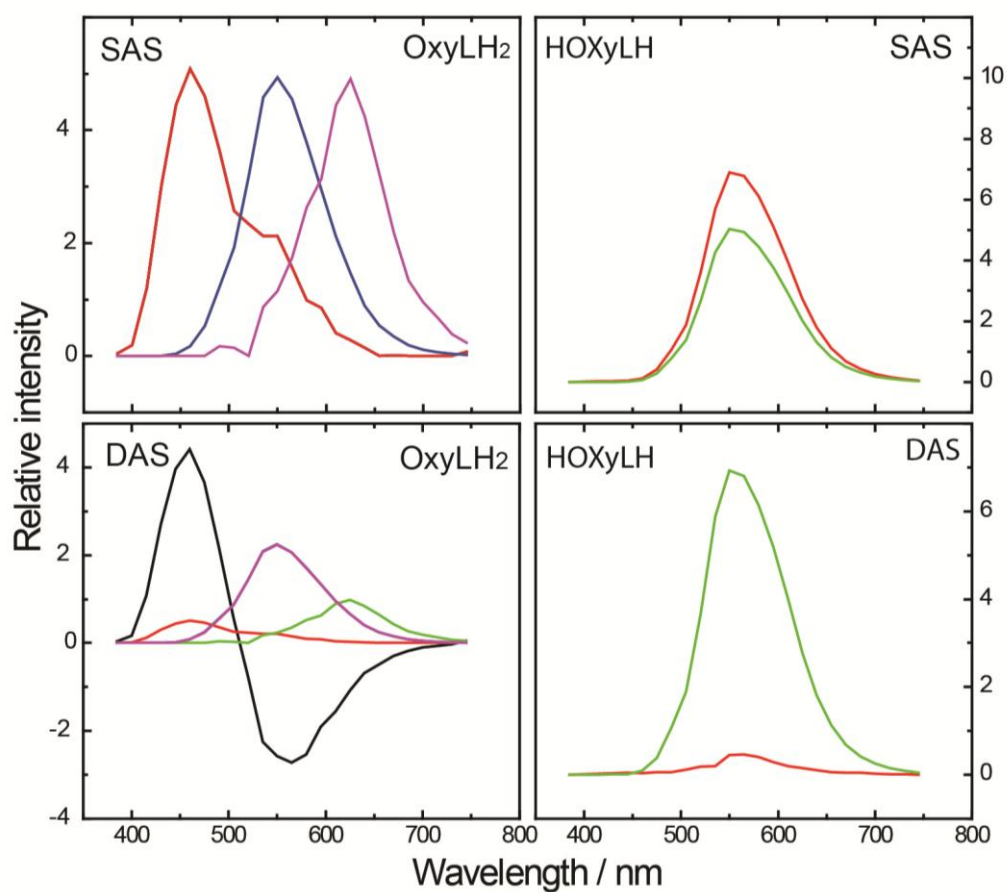


**Figure S6.** Global analysis results for oxyluciferin (OxyLH<sub>2</sub>) and 6'-dehydroxylated oxyluciferin (HOxylH) in water.

## Target analysis of the Oxy/H<sub>2</sub>O system

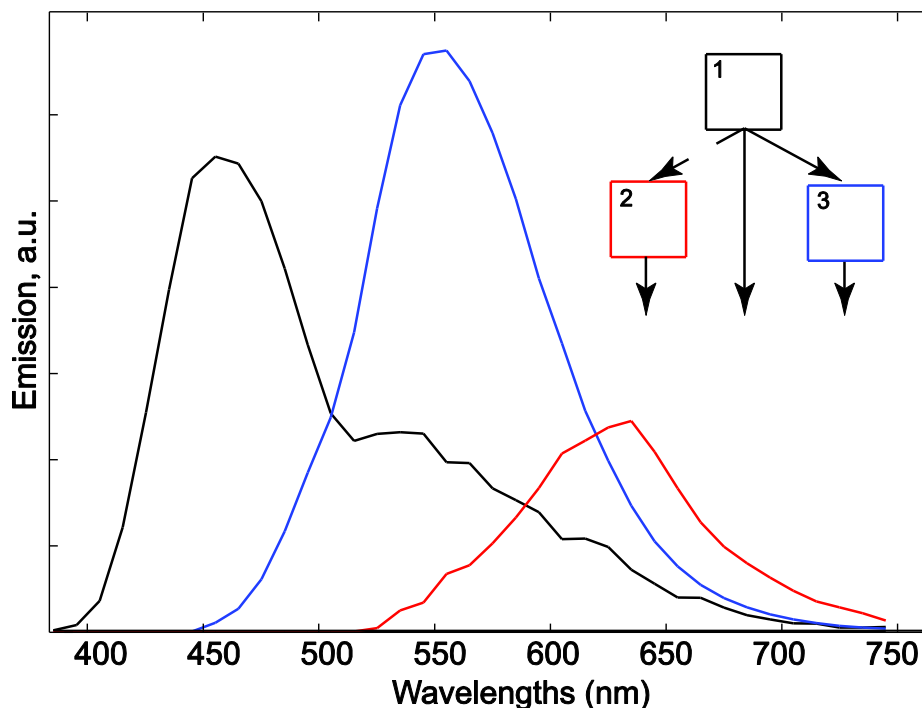


**Figure S7.** SAS of OxyLH<sub>2</sub> in water with the kinetic scheme resulted from target analysis.

Several target models were tested. The simplest and the best-fit one resulted in the following kinetic scheme.

Excitation came to state 1 (and compartment 2) with present time resolution it's impossible to resolve if state 2 is excited directly from ground state or formed from component 1 within few ps.

State 1 (black) decays bi-exponentially. The fast part has lifetimes of 0.060 ns (90%) and 0.3 ns (10%) (the errors in the starting concentrations is about 10%). Within 60 ps it excites states 3 and 2 (with present time resolution it's impossible to resolve if component 2 is excited directly from the ground state or it is formed from component 1 within few ps). The biexponential decay of 1 is probably caused by the geminate recombination described in the main text.

State 2 (red) decays with the lifetime of 0.52 ns

State 3 (blue) decays bi-exponentially with lifetimes of 2.7 ns (main decay time) and 7.7 ns. The biexponential decay of 1 is probably caused by the geminate recombination described in the main text.

According to this scheme we attribute 1 to neutral phenol-enol, 3 – to phenol-enolate. The assignment of 2 is more challenging. We tentatively attribute this emission at 630 nm to the formation of phenolate-enolate species. More detailed investigation of the spectral nature of this transient species is underway.



## H/D isotope effects on the OxyLH<sub>2</sub> fluorescence decay in water

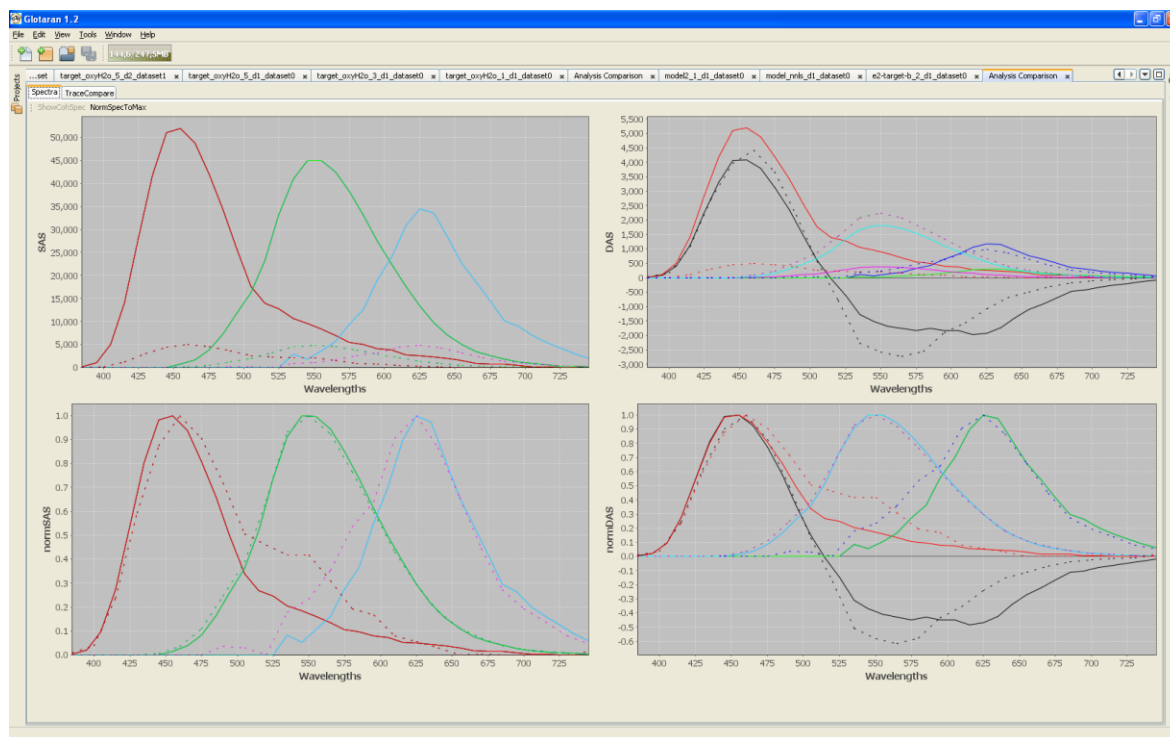


**Figure S8.** Screenshot of the fitting of spectra of **OxyLH<sub>2</sub>** in water and in D<sub>2</sub>O using the Glotaran software. Relative (top row) and normalized (bottom row) SAS and DAS. Solid lines – D<sub>2</sub>O data, dashed lines – H<sub>2</sub>O data.

Same target analysis was applied for both **OxyLH<sub>2</sub>**/D<sub>2</sub>O and **OxyLH<sub>2</sub>**/H<sub>2</sub>O systems (see previous page). In D<sub>2</sub>O State 1 decays bi-exponentially with lifetimes of 138 ps and 263 ps. The fast component excites states 2 and 3. Slow component is not capable to transform.

State 2 decays bi-exponentially with lifetimes of 0.45 ns and 1.2 ns.

State 3 decays bi-exponentially with lifetimes of 2.0 ns and 10 ns.

The pronounced H/D kinetic isotope effect (KIE) on the Component 1 decay (2.3 for the fastest component) supports our hypothesis that this process is mainly associated with the ESPT o water. This KIE was very close to that for the photoacids of comparable acidity.<sup>6</sup> An increase of the ESPT product lifetime in deuterated solvents is also a common phenomenon for various photoacids.<sup>7</sup>

<sup>6</sup> Huppert, D.; Tolbert, L. M.; Linares-Samaniego, S. *J. Phys. Chem. A* **1997**, 101, 4602.

<sup>7</sup> Solntsev, K. M.; Huppert, D.; Agmon, N.; Tolbert, L. M. *J. Phys. Chem. A* **2000**, 104, 4658.